International Journal of Biological Macromolecules 165 (2020) 63–70

Contents lists available at ScienceDirect

International Journal of Biological Macromolecules

journal homepage: http://www.elsevier.com/locate/ijbiomac

Succinyl chitosan gold nanocomposite: Preparation, characterization, in vitro and in vivo anticandidal activity

S.H.S. Dananjaya [a], S.L. Edirisinghe [b], N.T. Thu Thao [a], R. Saravana Kumar [c], H.M.S.M. Wijerathna [d], Ajith Yapa Mudiyanselage [e], Mahanama De Zoysa [b], Dongrack Choi [a,*]

[a] Zerone Bio Inc, 3rd Floor, Sanhak Building, Dankook University, Dandae-ro 119, Dongnam-gu, Cheonan Si, Chungcheongnam-do 31116, Republic of Korea
[b] College of Veterinary Medicine, Chungnam National University, Yuseong-gu, Daejeon 34134, Republic of Korea
[c] Department of Physics, Periyar University Constituent College of Arts and Science, Idappadi, Salem 637102, Tamil Nadu, India
[d] Department of Aquaculture and Aquatic Resources Management, University College of Anuradhapura, Sri Lanka
[e] Department of Chemistry, Faculty of Science, University of Ruhuna, Matara, Sri Lanka

ARTICLE INFO

Article history:
Received 14 July 2020
Received in revised form 1 September 2020
Accepted 17 September 2020
Available online 22 September 2020

Keywords:
N-succinyl chitosan
Gold nanocomposite
Antifungal activity
Candida albicans
Zebrafish

ABSTRACT

Herein, we have successfully synthesized a novel *N*-Succinyl chitosan/gold nanocomposite (*N*-SuC/Au NC) using *N*-SuC and gold(III) chloride, and investigated the biocompatibility and antifungal activity. The synthesized *N*-SuC/Au NC was characterized by UV–visible spectroscopy, X-ray diffraction, field emission scanning electron microscope, and inductively coupled plasma atomic emission spectroscopy. The *N*-SuC/Au NC exhibited a strong inhibition effect towards pathogenic *Candida albicans*. Morphological analysis revealed the destruction of *C. albicans* cell membrane due to *N*-SuC/Au NC treatment. The *in vitro* and *in vivo* toxicity of *N*-SuC/Au NC was analyzed with HEK293T mammalian cells and zebrafish larvae, respectively. The synthesized *N*-SuC/Au NC demonstrated no cytotoxicity towards HEK293T cells up to 1200 μg/mL concentration. The survival rate of the zebrafish larvae at 120 hpf, was found as 100% up to 1200 μg/mL of *N*-SuC/Au NC exposure. The *in vivo* studies further confirmed the inhibitory effects of *N*-SuC/Au NC on the formation of *C. albicans* hyphae in infected zebrafish muscle tissue.

1. Introduction

Mortality from fungal infection poses a significant health threat with higher mortality from systemic infections than that of bacterial species [1]. *Candida albicans* is the fourth most common pathogen responsible for infections, and has the ability to produce robust biofilms on medical devices, which is the key for pathogenesis [2]. *C. albicans* is a risk-free commensal and a human fungal pathogen which causes mucosal, cutaneous and systemic infections in immune compromised patients undergoing long-term treatment with antifungal agents [3]. Side effects from the present treatment regimens and the emergence of multi-drug resistance create complications in efficient therapy against the infections caused by *C. albicans* [4]. Hence, the development of novel therapeutic agents for the treatment of Candida infections is utmost important.

Chitosan, a deacetylated form of chitin, is the second-most naturally abundant co-polysaccharide next to cellulose [5]. There are many active amino and hydroxyl groups in chitosan, which react easily with a variety of chemical groups. The complex structure of chitosan results in poor water solubility, which greatly limits its application [6]. Molecular weight reduction and introduction of hydrophilic groups by chemical modification are well-known processes to improve the solubility, chemical reactivity and bioactivity of chitosan [5,7]. *N*-succinyl-chitosan (*N*-SuC) is a water soluble chitosan derivative obtained by the reaction of chitosan with succinic anhydride, through the introduction of carboxyl groups into chitosan *N*-terminal of the glucosamine units [8]. It possesses greater biocompatibility, moisture retention, low toxicity, and it is being used in many fields such as wound dressing, drug release, anticancer drug carriers, cosmetics and enzyme fixation [9]. Very recently, *N*-SuC immobilized lysozyme was used as an antimicrobial agent in strawberry preservation [10].

Metal nanoparticles (NPs) and metal nanocomposites (NCs) have received great interest in both the scientific and technological aspects over the last two decades [11]. Metal NC showed excellent chemical stability and biocompatibility due to their outstanding synergistic effects. Especially, metal-chitosan NC based on silver (Ag), gold (Au), platinum (Pt), and palladium (Pd) showed potent antimicrobial agent due to co-utilization of the antimicrobial properties of both chitosan and metal NPs. For example, the composite form of Ag NPs with polymer based matrix such as chitosan possesses enhanced antimicrobial properties at lower concentration with reduced toxic effects [12]. Hence, the development of biodegradable NC with minimum adverse effect on the host

* Corresponding author.
E-mail address: drchoi@zeronebio.com (D. Choi).

https://doi.org/10.1016/j.ijbiomac.2020.09.126
0141-8130/

and on the environment is important. Accordingly, in the present work, we have synthesized *N*-succinyl-chitosan gold nanocomposites (*N*-SuC/Au NC) without adding any reducing agents and investigated the antifungal activity against *C. albicans*. Also, the cytotoxicity of *N*-SuC/Au NC was analyzed using human embryonic kidney (HEK293T) cells. The *in vivo* toxicity was analyzed using zebrafish (*Danio rerio*) embryos. Also, the *in vivo* antifungal activity of *N*-SuC/Au NC was tested using *C. albicans* infected zebrafish by performing histopathological studies.

2. Materials and methods

2.1. Preparation of N-SuC and N-SuC/Au NC

The synthesis of *N*-SuC was carried out according to the previous report with slight modifications [13]. Briefly, 4 g of chitosan (Sigma Aldrich, USA) was dissolved in 100 mL of 3% (v/v) aqueous HCl solution at ambient temperature. Subsequently, 2 g of succinic anhydride (Sigma Aldrich, USA) was dissolved in 20 mL of pyridine and then, added dropwise to the chitosan solution under vigorous stirring. After 6 h, the pH of the reaction was raised to 8 by dropwise addition of NaOH (3 M) solution. Finally, the reaction was terminated by adding 120 mL of absolute ethanol. The precipitate was filtered and washed several times with ethanol and dried in vacuum at 50 °C. The final product (4 g) was purified by dissolving it in 100 mL of distilled water and filtering through 1 μm Whatman® filter paper. The filtered solution was re-precipitated by adding 100 mL of ethanol. Finally, the precipitate was filtered and washed in sequence with ethanol and acetone, and dried in vacuum at 50 °C to obtain *N*-SuC.

For the synthesis of *N*-SuC/Au NC, 20 mg/mL of *N*-SuC and 4 mM $HAuCl_4 \cdot 3H_2O$ solutions were prepared using Milli-Q (Millipore) water. After that, 20 mL of *N*-SuC solution was mixed with 2 mL of $HAuCl_4 \cdot 3H_2O$ solution and the mixture were heated in a water bath at 90 °C for about 5 min. The color of the reaction mixture was changed from pale yellow to purple red, indicating the formation of Au NPs. Then, the reaction mixture was stirred for 10 min, and equal volume of ethanol (22 mL) was added to precipitate the *N*-SuC/Au NC. Finally, the precipitate was filtered and washed with ethanol and dried in vacuum oven at 50 °C for 6 h.

2.2. Characterization of N-SuC and N-SuC/Au NC

The ^1H nuclear magnetic resonance (NMR) spectra of chitosan and *N*-SuC were acquired using NMR system (Bruker, Germany) at 400 MHz. D_2O/CD_3COOD was used as solvent and the chemical shifts (δ) were reported in parts per million (ppm) using tetramethylsilane (TMS) as an internal reference. The degree of substitution of *N*-SuC was determined by the potentiometric titration method [14]. Briefly, 5 mg/mL of *N*-SuC aqueous solution was prepared first and then, 3 M HCl was added dropwise to adjust the pH of the solution to 2. This acidic solution was titrated against 0.1 M NaOH. The degree of substitution was calculated using the formula,

$$DS = (177-A)/(mN-SuC-101\ X\ A).A = V_{NaOH}\ X\ C_{NaOH}$$

where, C_{NaOH} and V_{NaOH} are the concentration and volume of NaOH, respectively. m*N*-SuC is the mass of *N*-SuC. The molecular weights of glucosamine and succinyl group are 177 and 101, respectively.

X-ray diffraction (XRD) analysis was carried out using Bruker D8-Advance (USA) X-ray diffractometer with Cu Kα radiation (λ = 1.544 Å). The optical properties were studied by UV–vis absorption spectra recorded using a spectrophotometer (Mecasys, Korea) in 325–600 nm wavelength range. The surface morphology was analyzed using a field emission scanning electron microscope (FESEM, SEISS SIGMA 500, SEISS, Germany). For FESEM analysis, the N-Suc/Au NC powder was placed on conductive carbon adhesive tape and coated with osmium using an ion sputter (E-1030, Hitachi, Japan). The amount of Au in the synthesized *N*-SuC/Au NC was determined by inductively coupled plasma atomic emission spectroscopy (ICP-AES, Perkin-Elmer Optima, USA). A known amount of the synthesized *N*-SuC/Au NC was dissolved in ultra-high pure HNO_3, to determine the Au content. The solubility of *N*-SuC/Au NC was evaluated at different pH from transmittance measurements at 600 nm [15]. For transmission measurements, *N*-SuC/Au NC was dissolved in 1% acetic acid (5 mg/mL) and the pH of the solution was adjusted to different values with the addition of 5 M NaOH solution. The *N*-SuC/Au NC was considered to be insoluble when the transmittance of the *N*-SuC/Au NC solution was less than 50% of the transmittance for aqueous media at different pH. The pH-dependent charge profile was monitored by evaluating the zeta potential (S-90, Malvern Instruments Ltd.,UK) of *N*-SuC/Au NC solution (1 mg/mL) at various values ranging from 3 to 11.

2.3. Culture conditions of C. albicans

C. albicans strains (KCTC 27242) were purchased from the Korean Collection for Type Culture. A single colony picked up from the fresh potato dextrose agar (PDA) plate was cultured in potato dextrose broth (PDB) under aerobic conditions at 30 °C for 24 h in a shaking incubator at 180 rpm. To harvest the *C. albicans* cells, well grown culture media were centrifuged at 3500 rpm for 10 min and washed twice with phosphate buffered saline (PBS, pH ~ 7.4) followed by re-suspension in PBS (OD_{600} ~ 0.1) to adjust the desired concentration of 10^6 colony-forming units per milliliter (CFU/mL), which was calculated using a hemocytometer.

2.4. In vitro anticandidal activity of N-SuC and N-SuC/Au NC

The in vitro anticandidal activity of *N*-SuC and *N*-SuC/Au NC against *C. albicans* was investigated by broth dilution procedure [16]. *C. albicans* were treated with different concentrations of ***N*-**SuC and *N*-SuC/Au NC. Nystatin (10 μg/mL) was used as a positive control. The lowest concentration at which no observable *C. albicans* growth occurs characterizes its minimum inhibition concentration (MIC) value. Also, the minimum fungicidal concentration (MFC) was determined by sub-culturing 10 μL of the medium collected from the wells on PDA medium plates. The MFC was the lowest concentration that yielded no colonies after 24 h growth on the agar.

2.5. C. albicans growth curve studies

The *C. albicans* cells were revived freshly by a subculture on a PDA plate. A loopful of inoculum was introduced into the PD broth and the cells were grown at 30 °C for 16 h before use. Various concentrations of *N*-SuC/Au NC (0–32 μg/mL) were separately added into the conical flasks comprising of the inoculated medium (*C. albicans*; 10^6 CFU/mL), which was incubated at 30 °C in a shaking incubator (180 rpm). Nystatin (10 μg/mL) was used as a positive control. The growth level of *C. albicans* was monitored at prearranged time periods (0, 3, 6, 9, 12, 15, 18, and 21 h) after incubation with agitation at 30 °C. 1 mL aliquot from each sample in a conical flask was removed and the growth was observed turbidometrically at 600 nm using a microplate reader (Bio-Rad, USA). The optical densities were recorded for each concentration with respect to time, and all the time-kill curve experiments were performed in triplicates.

2.6. Morphological analysis of N-SuC/Au NC treated C. albicans

The morphological changes of *C. albicans* due to *N*-SuC/Au NC treatment was investigated according to the reported method [17]. Briefly, *C. albicans* cells (10^6 CFU/mL) were incubated with *N*-SuC/Au NC (16 and 32 μg/mL) at 30 °C for 12 h with an orbital shaking of 180 rpm. After incubation, the *C. albicans* cells were washed several times with PBS and fixed in 2.5% glutaraldehyde for 30 min. The pre-fixed cells were again

washed using PBS and dehydrated by increasing concentrations of ethanol, consisting of 30, 50, 70, 90, and 100% for 10 min, twice. The dehydrated cells were dried and coated with platinum using an ion sputter (E-1030, Hitachi, Japan) and the morphological changes was analyzed using ultra-high resolution FESEM.

2.7. Effect of N-SuC/Au NC on the membrane permeability of C. albicans

The membrane permeability of *C. albicans* cells exposed to *N*-SuC/Au NC was examined as described in our previous work [18], using propidium iodide (PI, Sigma Aldrich, USA). Briefly, cell suspensions of the control and *N*-SuC/Au NC treated samples (16 and 32 μg/mL) were centrifuged (5000 rpm for 2 min) and the pellets were resuspended in PBS. The treated cells were incubated with 5 μg/mL of PI at 30 °C for 15 min in the dark and then over staining were washed twice with PBS. Finally, one drop of each suspensions was placed on the cover slip and the fluorescence images were recorded using a Carl Zeiss LSM 5 Live confocal laser scanning microscope (CLSM) scan head integrated with the Axiovert 200 M inverted microscope (Carl Zeiss, Jena, Germany).

2.8. Safety assessment of N-SuC/Au NC

The *in vitro* cytotoxicity of *N*-SuC/Au NC was studied on HEK293T (human embryonic kidney, ATCC-11268) cells using WST-8 cell viability assay kit (Quanti-Max™, Korea). HEK293T cells (1×10^4 cells/well) were seeded into a 96 well plate with the high-glucose Dulbecco's Modified Eagle's Medium (DMEM, Invitrogen, USA) with 1% antibiotic/antimycotic solution (Gibco, USA) and 10% fetal bovine serum (FBS) (Hyclone, USA). After 24 h, cells were treated with different concentrations (0–2000 μg/mL) of *N*-SuC/Au NC. After 24 h of incubation, WST-8 reagent (20 μL) was added to each well and incubated at 37 °C for 3 h with 5% CO_2. The optical density (OD) was measured using microplate reader (Bio-Rad, USA) at 450 nm. The cell viability was estimated using the formula,

$$\text{Cell viability } (\%) = (\text{ODS}/\text{ODC}) \times 100,$$

where, *ODS* and *ODC* are the mean values of the sample wells and the control, respectively.

The *in vivo* toxicity of *N*-SuC/Au NC was determined using zebrafish embryo. The two to three hours post-fertilization (hpf) mature eggs (6 per well) were seeded into 12 well plates. These wells were then filled with E3 embryo medium (0.059 M NaCl, 0.00067 M KCl, 0.00076 M $CaCl_2$ and 0.0024 M $NaHCO_3$; pH 6.5–7.0) and treated with various concentrations of *N*-SuC/Au NC (namely 250, 500, 750, 1000, 1250, 1500, 1750, and 2000 μg/mL). The eggs were regularly monitored for the phenotypic response for 120 hpf in a stereo-microscope (Nikon, SMZ1000, Japan). The survival rate was determined by identifying the mortality of the zebrafish embryos (complete loss of mobility in zebrafish embryo, coagulation of the unhatched eggs or no hatching even after 72 hpf) in the presence of various concentrations of *N*-SuC/Au NC at time intervals of 24 hpf.

2.9. In vivo efficacy of N-SuC/Au NC upon C. albicans infection in zebrafish model

The antifungal activity of *N*-SuC/Au NC against *C. albicans* infection was investigated using zebrafish model as described in our previous work [19]. Wild-type AB zebrafish fish line (5 months old) were maintained at standard culture conditions [20]. In brief, 90 fish (0.50 ± 0.08 g) were anesthetized by immersing in 0.17 g/mL of tricaine (Sigma, USA) solution and randomly divided into three groups with 3 replicates ($n = 30$/replicate). At the day of experiment, *C. albicans* (3 μL) was intramuscularly injected at a dose of 3×10^6 cells/fish (3 μL) using Hamilton® syringe, and the injected fish were immediately put into recovery tanks (4 L). After 12 h post infection (hpi), individual fish were treated with 32 μg of *N*-SuC/Au NC, 10 μg of nystatin as positive control and 3 μL of PBS for negative control. The procedure was repeated after every 12 h intervals until 120 hpi, and the cumulative mortality was measured throughout the experimental time.

Examination of *C. albicans* infection was monitored through histological analysis in zebrafish at 72 hpi. Euthanized whole fish with an overdose treatment of tricaine were fixed in 10% neutral buffered formalin. After 24 h, the fish were washed with PBS for 12 h, and decalcification was done with decalcifying solution Lite (Sigma, USA) using manufacture's protocol (50 mL/fish) for 3 days. Thereafter, the fish were washed with PBS for 12 h, and the infected site was separated and processed under tissue processor (Leica® TP1020 Semienclosed Benchtop Tissue Processor, Germany) for 12 h. After processing, paraffin embedding was continued (Leica® EG1150 Tissue Embedding Center, Germany), and sectioned into 5 μm thickness (Leica® RM2125 microtome, Germany). After deparaffinization and dehydration, the infection of *C. albicans* was examined by staining serial transverse tissue sections with Periodic Acid-Schiff stain (PAS). First, the sections were treated with 0.5% periodic acid for 5 min followed by Schiff's solution for 20 min. After washing, the sections were again treated with Gill's hematoxylin for the counter staining. The infections were observed through Leica® microscope (3000 LED, Germany) and the images were captured by Nikon Eclipse 80i (Nikon Corporation, Japan).

3. Results and discussions

3.1. Characterization of N-SuC and N-SuC/Au NC

The *N*-SuC was prepared *via* ring-opening reactions with succinic anhydride in the presence of pyridine. Carbonyl carbon of succinic anhydride is a strong electrophile which readily reacts with the nucleophilic amine groups of chitosan [21]. Pyridine was added as an acylation catalyst to promote the amine/anhydride acylation reaction [22]. The percentage yield for 2:1 weight ratio of chitosan and succinic anhydride was 88.25 ± 2.56%. The ^{1}H NMR spectra of chitosan and *N*-SuC are given in Fig. 1. The ^{1}H NMR spectrum of chitosan showed signals at $\delta = 3.15$ (H2 of glucosamine); $\delta = 3.44$–4.30 (H2 of *N*-acetyl glucosamine, H3, H4, H5, and H6), and $\delta = 4.88$ (H1). On the other hand, the ^{1}H NMR spectrum of *N*-SuC showed a new signal at $\delta = 2.25$–2.50 ppm ($NH—CO—CH_2CH_2—COOH$ of succinyl group) in addition to the chitosan signals, indicating the successful formation of *N*-SuC. The ^{1}H NMR spectral characteristics of the synthesized *N*-SuC were identical to the previous reports [23,24].

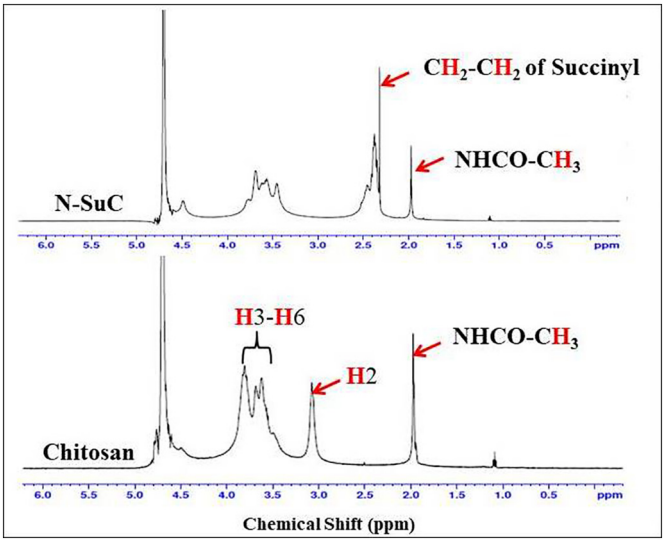

Fig. 1. ^{1}H NMR spectra of chitosan and *N*-SuC.

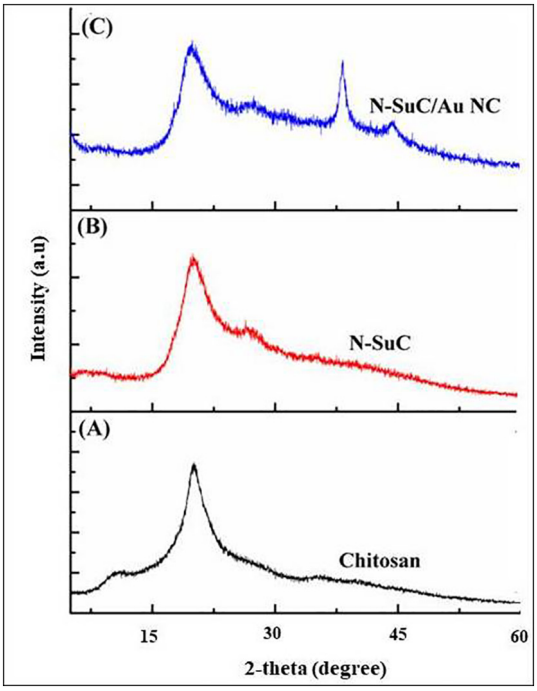

Fig. 2. XRD spectra of (A) chitosan, (B) *N*-SuC and (C) *N*-SuC/Au NC.

Fig. 2 shows the XRD spectra of chitosan, *N*-SuC and *N*-SuC/Au NC. The XRD spectrum of chitosan (Fig. 2A) showed two distinct crystalline peaks at around 10° and 20°, attributed to the strong intermolecular and intramolecular hydrogen bonds between hydroxyl and amino groups of chitosan [25]. The '*H*' bond might support certain structural regularity in chitosan to form crystalline regions and insolubility in water. In case of *N*-SuC (Fig. 2B), the diffraction peak at 10° disappeared and the peak intensity of diffraction peak at 20° lowered, which indicates the destruction of the intermolecular 'H' bonds and the crystalline regions of chitosan due to successful substitution of succinyl group. The XRD pattern of *N*-SuC/Au NC (Fig. 2C) showed major diffraction peaks at 38.56°, 44.38°, 64.72° and 77.28° corresponding to the (111), (200), (220) and (311) crystalline planes, respectively, of the face centered cubic (FCC) structure of Au (JCPDS card no. 04-0783). The broad hump at 20.33° corresponds to the amorphous structure of *N*-SuC. The diffraction pattern of Au and allomorphic character of chitosan were consistent with the previous report of chitosan gold nanocomposite [18]. Due to its electronegative property chitosan is generally used as a reducing agent for preparing Au NPs. The presence of amino group in the polyatomic structure of chitosan delivers steric hindrance and stabilizes the Au NPs [26,27]. The degree of substitution of succinyl group during the reaction for 2:1 weight ratio of chitosan and succinic anhydride was found to be 0.68 ± 0.08. This indicates that the residual $-NH_2$ groups in the glucosamine unit act as an electrostatic stabilizer of Au NPs during the formation in N-SuC/Au NC.

The UV–vis absorption spectrum, FESEM, solubility and zeta potential measurements are given in Fig. 3. The UV–vis absorption spectra (Fig. 3A) of *N*-SuC and *N*-SuC/Au NC solutions displayed different absorption profiles. The *N*-SuC solution did not show any notable peak between the wavelength range 325–600 nm, while the *N*-SuC/Au NC exhibited a clear absorption peak around 520 nm. This strong absorption band at 520 nm originates from the surface plasmon of the Au NPs. The inset in Fig. 3A shows the appearance of the synthesized compounds aqueous solution. As shown in figure, the pale-yellow color of

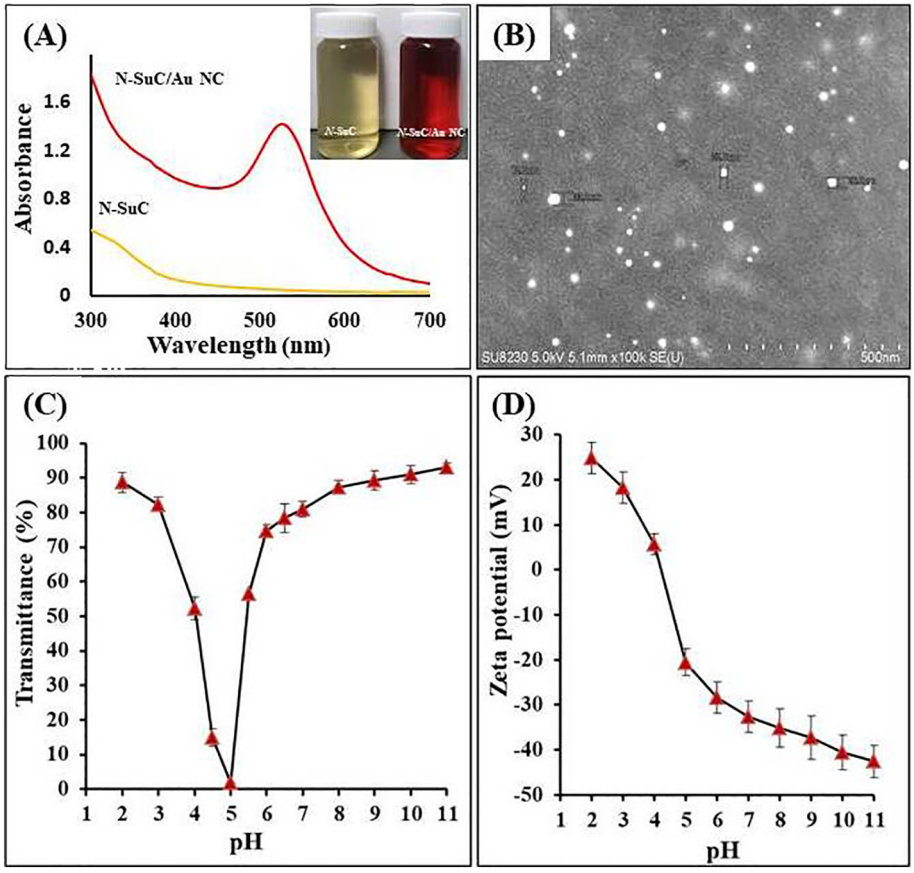

Fig. 3. (A) UV–Vis spectrum of *N*-SuC and *N*-SuC/Au NC. Inset in (A) is the photographic images of *N*-SuC and *N*-SuC/Au NC aqueous solutions, (B) FESEM of *N*-SuC/Au NC, (C) solubility profile of *N*-SuC/Au NC at various pH, and (D) zeta potential of *N*-SuC/Au NC at various pH.

N-SuC solution transformed to ruby-red due to the formation of *N*-SuC/Au NC. The FESEM image (Fig. 3B) showed spherical shaped Au NPs with an average diameter of 22 nm uniformly distributed on the surface of *N*-SuC. The size and morphology of the Au NPs play an important role in the antifungal activity. For example, it was reported that the smaller sized gold nanodiscs exhibit more fungicidal activity than the large sized gold polyhedral nanocrystals [28]. The ICP-AES analysis confirmed that *N*-SuC/Au NC contains 1.46 ± 0.21% of Au.

The solubility of *N*-SuC/Au NC was determined by transmittance measurement for various pH at 600 nm. Fig. 3(C) shows the solubility of *N*-SuC/Au NC both in the basic (pH > 7) and acidic regions (pH < 7). The solubility of *N*-SuC/Au NC in acidic region was attributed to the protonation of amino group (-NH_2 to –NH_3^+) and the solubility in alkaline region was caused by the change of carboxylate group to carboxylate ion (-COOH to –COO^-). The insolubility region between pH ~ 4.5–5.5 was attributed to the isoelectric point which exists equimolar of –NH_3^+ and–COO^- group in the *N*-SuC/Au NC molecule. The zeta potential measurement (Fig. 3D) revealed that *N*-SuC/Au NC exhibits a net positive charge of the surface at pH < 4 due to the protonation of -NH_2 group. The negative zeta potential at basic pH was attributed to the deprotonation of -COOH groups. Similar solubility profile and pH dependent charge profiles in Zeta potential measurements have been reported for *N*-SuC [24,29].

3.2. Anticandidal activity of N-SuC/Au NC

The MIC and MFC values of *N*-SuC/Au NC were determined to understand the growth inhibition of *C. albicans*. The synthesized *N*-SuC did not show anticandidal activity against *C. albicans* up to 6 mg/mL. Previous report on *N*-SuC (4 mg/mL) also did not show any anticandidal activity against clinically isolate ten *C. albicans* strain from oral rinse samples of healthy individuals [30]. The MIC and MFC level of *N*-SuC/Au NC against *C. albicans* were found to be 16 and 32 μg/mL, respectively. The time-kill kinetic analysis clearly showed growth inhibition of *C. albicans* by *N*-SuC/Au NC above the MIC level similar to the positive control nystatin (Fig. 4A). At lower *N*-SuC/Au NC concentrations (4 and 8 μg/mL) below the MIC level a partial growth inhibition was observed. The synthesized *N*-SuC/Au NC demonstrated better anticandidal activity when compared to the chitosan-Au NC which exhibited MIC and MFC values of 50 and 75 μg/mL, respectively, against the same *C. albicans* strain [18]. Au NPs with MIC and MFC values of 24.37 and 97.5 μg/mL, respectively, were reported previously for the growth inhibition of fluconazole-resistant strains of *C. albicans* [31]. Also, the commercially available Au NPs (30 nm) was reported to have growth inhibitory effect on *C. albicans* at 32 μg/mL concentration [32]. Comparing with these earlier reports, it can be deduced that the synthesized *N*-SuC/Au NC can be a potent anticandidal agent.

The cell viability of *C. albicans* was determined by MTT assay after the treatment with different concentrations of *N*-SuC/Au NC (0–32 μg/mL). The cell viability (Fig. 4B) decreased ($p < 0.05$) significantly due to *N*-SuC/Au NC treatment, and exhibited a concentration dependent profile. The control (without *N*-SuC/Au NC) exhibited

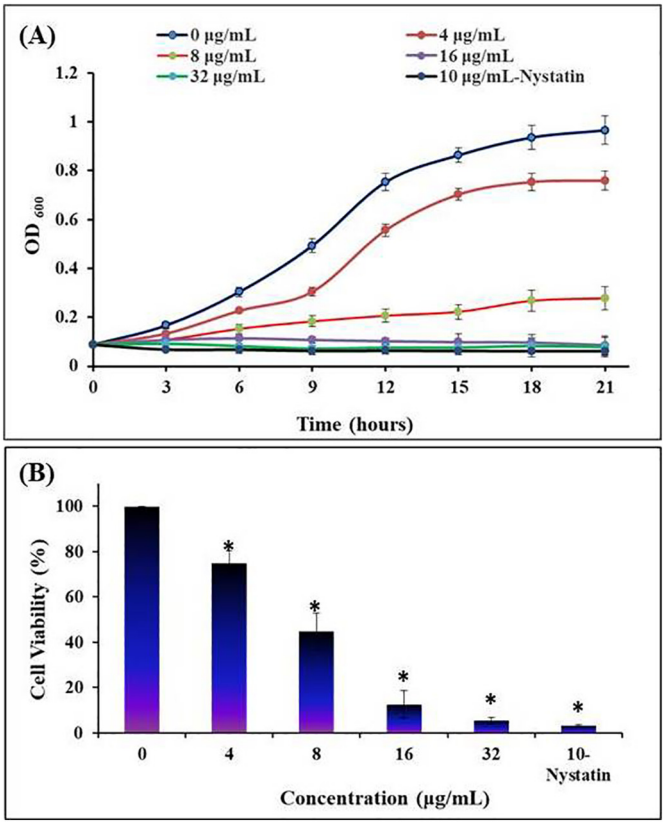

Fig. 4. (A) Growth performance and (B) cell viability of *C. albicans* exposed to different concentrations of *N*-SuC/Au NC. (A) In growth inhibition assay, cell growth was assessed after treatment with *N*-SuC/Au NC at 30 °C by measuring the OD at 600 nm at every 3 h intervals. The bars indicate the S.D. ($n = 4$). (B) Cell viability was assessed after treatment with different concentration of *N*-SuC/Au NC. Significant differences in *C. albicans* cells viability were obtained with respect to untreated controls ($P < 0.05$). The treatments with*mark represent the significant cell viability (%).

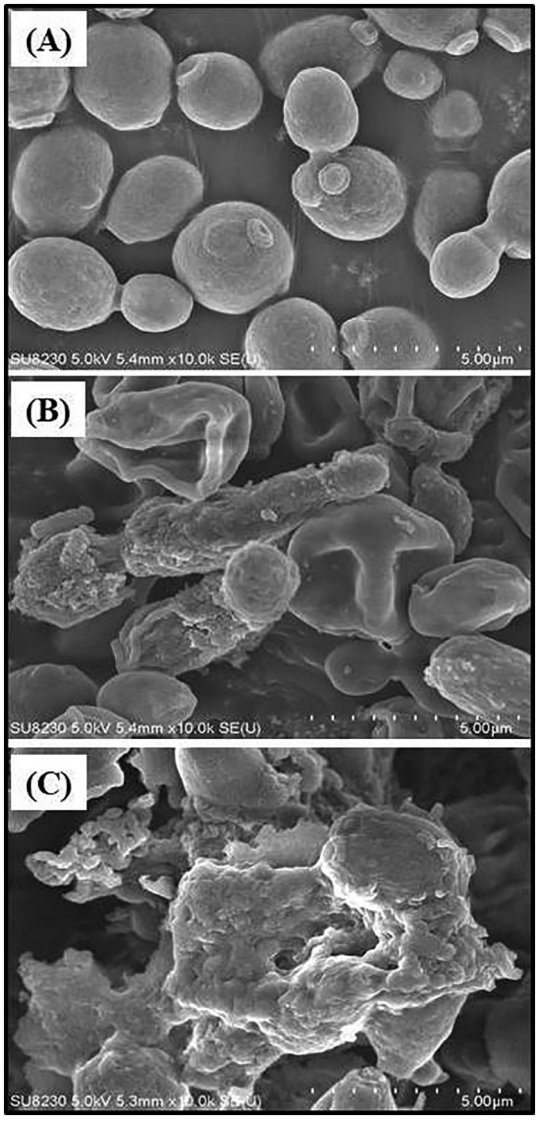

Fig. 5. FESEM images of *C. albicans* (A) control (untreated) cells; (B) 16 μg/mL and (C) 32 μg/mL of *N*-SuC/Au NC treated cells.

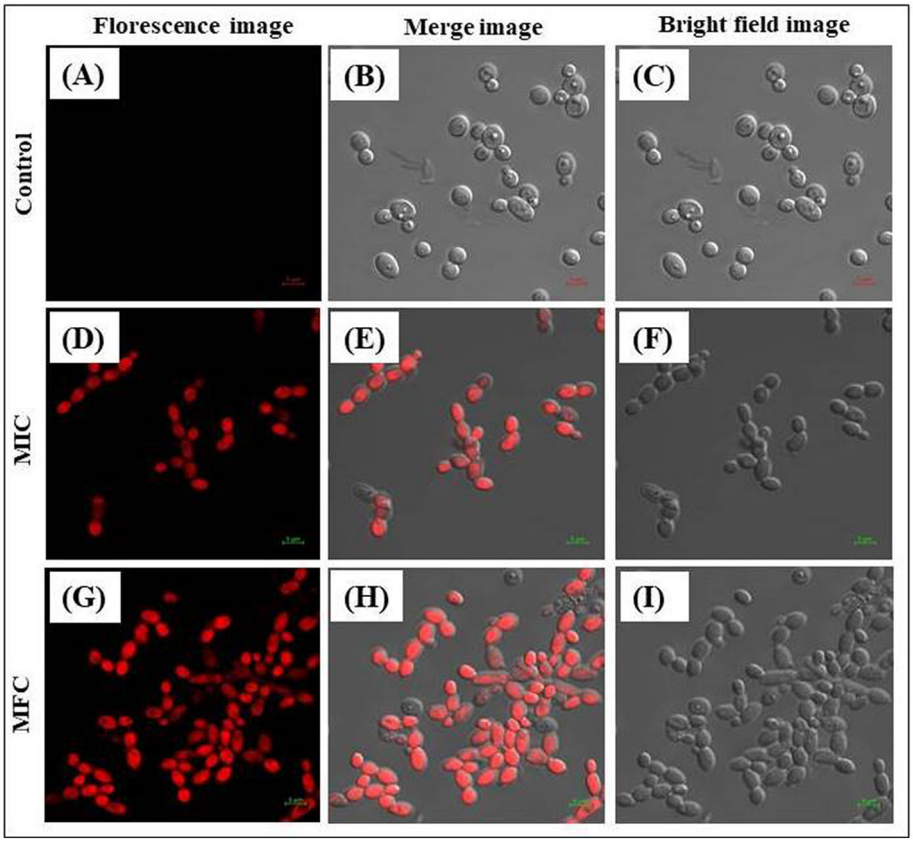

Fig. 6. CLSM image of PI strained *N*-SuC/Au NC treated *C. albicans* cells: (A)–(C) control (untreated cells); (D)–(F) treated at MIC (16 μg/mL); and (G)–(I) treated at MFC (32 μg/mL).

maximum cell viability. The cell viability decreased with the increase in NC concentration and reached a minimum of 5.35% at the MFC (32 μg/mL) level concentration of *N*-SuC/Au NC. The nystatin treatment (10 μg/mL) showed 2.58% cell viability.

3.3. Morphological analysis of N-SuC/Au NC treated C. albicans

The effect of *N*-SuC/Au NC on the membrane structure of *C. albicans* was investigated by FESEM. As anticipated, the ultra-structural analysis (Fig. 5) clearly showed the changes in the morphology of *C. albicans* membrane after the treatment with *N*-SuC/Au NC at the MIC (16 μg/mL) and MFC (32 μg/mL) level concentrations. The untreated *C. albicans* cells (Fig. 5A) displayed a smooth and undamaged cell surface. In contrast, the *N*-SuC/Au NC treated *C. albicans* cells showed severely damaged and irregular shaped cells with swollen and rough membrane of *C. albicans* cells, at the MIC (16 μg/mL, Fig. 5B) and MFC (32 μg/mL, Fig. 5C) level treatment. Ag- and Au-chitosan NC treated *C. albicans* have shown similar cell wall deformities and injuries at the MIC (50 μg/mL) and MFC (75 μg/mL) level treatments [18,19].

PI uptake assay was further conducted to comprehend the effect of *N*-SuC/Au NC on the permeability of *C. albicans* cell membrane and concomitant cell death. PI is a fluorescent molecule which has the ability to bind with the DNA. It shows zero penetration in live intact cell membrane. However, PI can penetrate the dead cells with high permeability due to damaged cell membrane and exhibit a red florescence inside the dead cells [33]. The CLSM images (Fig. 6) revealed the loss of *C. albicans* cell membrane integrity due to *N*-SuC/Au NC treatment. The control (*i.e.* untreated groups, Fig. 6A–C) did not show any red florescence indicating the intact cell wall structure of the *C. albicans*. In contrast, at the MIC level (Fig. 6D–F) treatment of *N*-SuC/Au NC both non-emitting and red florescence emitting cells were observed. At the MFC level (Fig. 6G–I) most of the *C. albicans* cells exhibited red florescence in the entire cell range owing to the greater membrane permeability. Taken together the FESEM and PI uptake analysis it can be concluded that *N*-SuC/Au NC has greater potential to damage and destruct the cell membrane of *C. albicans* and cause subsequent death.

3.4. Safety assessment of N-SuC/Au NC

Prior to the therapeutic application, the toxicity of the synthesized *N*-SuC/Au NC was tested with the mammalian cells and zebrafish larvae. The *in vitro* toxicity of *N*-SuC/Au NC was tested using HEK293T cells by WST-8 cell viability assay kit. The cytotoxicity results (Fig. 7A) showed no significant difference ($P < 0.05$) in the cell viability up to 1200 μg/mL of *N*-SuC/Au NC concentrations compared to the control. Also, the morphology of the cells remained intact when treated with *N*-SuC/Au NC up to 1200 μg/mL (Data are not shown). At higher concentrations (1400 μg/mL) a slight toxicity was observed. The green synthesized Au NPs showed more than 95% HEK293T cell viability only at low concentrations ranging from 100 to 500 μg/mL [34]. Hence, the cytotoxicity results indicate the biocompatibility of the synthesized *N*-SuC/Au NC. However, more experiments on other mammalian cells need as well to completely elucidate the cell cytotoxic effect of *N*-SuC/AuNC.

The *in vivo* toxicity of *N*-SuC/Au NC was analyzed by zebrafish embryo model. The survival rate of the zebrafish larvae at 120 hpf, in response to *N*-SuC/Au NC at various concentrations is given in Fig. 7(B). At lower *N*-SuC/Au NC concentrations (< 1200 μg/mL) the zebrafish survival rate at 120 hpf was found to be 100% and at higher concentrations (≥ 1600 μg/mL) the survival rate reduced below 50%. However, no malformation in zebrafish larva was observed up to 1400 μg/mL of *N*-SuC/Au NC concentration. Photographs comparing the malformations at high concentrations to the control group are presented in Fig. 7(C–G). Generally, the toxicity of the NPs relied not only on the administered

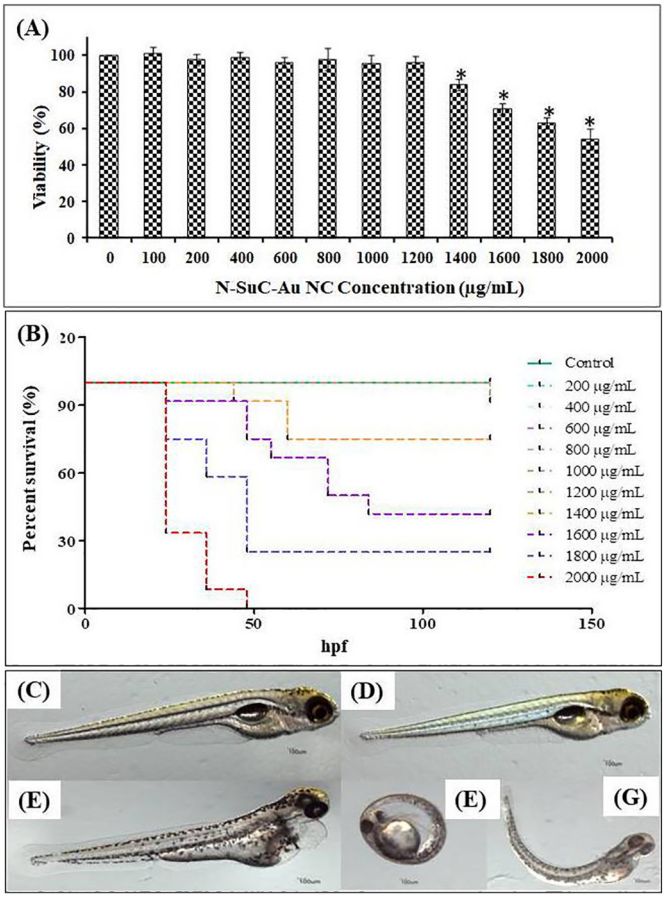

Fig. 7. Safety assessment of *N*-SuC/Au NC (A) effect of *N*-SuC/Au NC on the viability of HEK 293 T cells, (B) survival curve of zebrafish larvae after *N*-SuC/Au NC treatment, (C) zebrafish larvae at 120 hpf without treatment (D) zebrafish larvae treated with 1200 μg/mL *N*-SuC/Au NC at 120 hpf, (E) pericardial edema larvae treated with 2000 μg/mL *N*-SuC/Au NC, (F) unhatched embryo treated with 2000 μg/mL *N*-SuC/Au NC, and (G) spinal and tail deformation larvae treated with 2000 μg/mL *N*-SuC/Au NC.

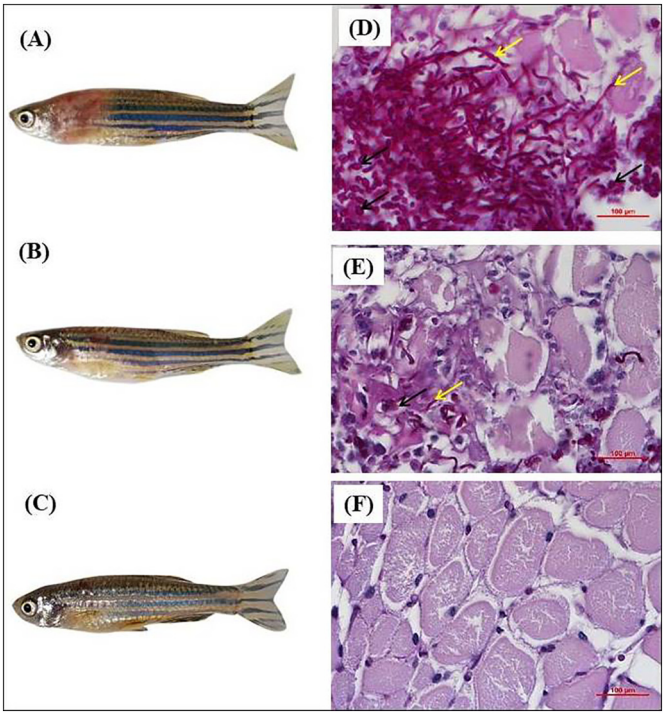

Fig. 8. Efficacy of *N*-SuC/Au NC therapy on *C. albicans* infection in zebrafish dorsal muscle at 72 hpi. (A) Control; (B) *N*-SuC/Au NC treated fish; (C) nystatin treated fish. Histopathological examination of *C. albicans* infection in zebrafish dorsal muscle tissue, the infected site showed the invading yeast-hyphae and inflamed tissues with cell infiltration (×400). (D) Control; (E) *N*-SuC/Au NC treated fish tissue; (F) nystatin treated fish tissue. The yellow and black arrows indicate *C. albicans* hyphae and cells, respectively.

dose but also on the size, shape, capping agent, particle stability and the quality of the aquatic medium [35].

3.5. Efficacy of N-SuC/Au NC therapy on C. albicans infection in zebrafish

In recent years, zebrafish model has been increasingly used for pathological research due to its genome similarity as a perfect host vertebrate and also as an assuring host system for *C. albicans* infection [19]. Accordingly, the efficacy of *N*-SuC/Au NC against *C. albicans* infection was examined using the zebrafish. After injecting *C. albicans* cells into the dorsal muscle at 72 hpi, the injected site (negative control) showed severe fungal growth (Fig. 8A) and revealed abnormal swimming behavior. The zebrafish moved under an upright position and gradually blocked their operculum. The group treated with *N*-SuC/Au NC (32 μg per fish) showed less visible fungal colonization at the injected site (Fig. 8B) compared to the PBS treated group, and the fungal colonization disappeared at 120 hpi (Data is not shown). Meanwhile, no fungal colonization was observed in nystatin treated group (positive control, Fig. 8C). The cumulative survival rate at 120 hpi was found to be 12% and 68% for the negative control and *N*-SuC/Au NC treated groups, respectively. Nystatin (10 μg per fish) treated group showed the highest survival rate of 82%. The lowering of the survival rate after the antifungal treatment may be attributed to the environmental stress and side effects of the antifungals.

The formation of colonies and invaded tissues by *C. albicans* at various anatomical sites including liver, gastrointestinal tract, connective tissue and muscles were observed in dead fishes after an infection dose of 1×10^8 CFU [36]. Similar pathological observations of *C. albicans* colonization and filamentation in the host tissues of mouse, human patients and zebrafish have also been reported [37,38]. Consequently, the colony formation and histopathological analyses inside the zebrafish due to *C. albicans* were examined. As shown in Fig. 8, the PBS treated group showed widespread growth of *C. albicans* hyphae and inflammatory cells (Fig. 8D) compared to the *N*-SuC/Au NC (Fig. 8E) and nystatin treated (Fig. 8F) groups. Hence, the results of *in vivo* study demonstrated the strong inhibition effects of *N*-SuC/Au NC on the growth of *C. albicans* in zebrafish muscles, indicating the anticandidal efficacy of the *N*-SuC/Au NC.

4. Conclusion

In the present work, we elucidated the antifungal activity and biocompatibility of *N*-SuC/Au NC. Succinyl group was introduced at the *N*-position of the glucosamine units of chitosan and subsequently synthesized *N*-SuC/Au NC without adding any reducing agents. The physiochemical characterization of the synthesized *N*-SuC/Au NC was performed using XRD, FESEM, UV–Vis absorption, ICP-AES, solubility and zeta-potential measurements. The *in vitro* anticandidal activity of *N*-SuC/Au NC investigated by turbidimetric assay demonstrated good inhibition property of the NC against *C. albicans*. FESEM analysis and PI uptake assays confirmed the cell membrane destruction due to *N*-SuC/Au NC treatment. Based on the experimental results, we conclude that the *N*-SuC/Au NC has strong anticandidal activity and possess good biocompatibility to be a potential antifungal agent against other pathogenic fungi.

Declaration of competing interest

All the authors in the manuscript will decelerated that no conflict of interest.

Acknowledgment

We greatly appreciate the technicians from Leaders in Industry-University Cooperation (LINC), Dankook University for their technical assistance.

References

[1] M.A. Pfaller, D.J. Diekema, Epidemiology of invasive candidiasis: a persistent public health problem, Clin. Microbiol. Rev. 20 (2007) 133–163.
[2] V. Kesarwani, H.G. Kelly, M. Shankar, K.J. Robinson, S.J. Kent, A. Traven, S.R. Corrie, Characterization of key bio-nano interactions between organosilica nanoparticles and Candida albicans, ACS Appl. Mater. Interfaces 11 (2019) 34676–34687.
[3] S. Khalid, S. Parveen, M.R. Shah, S. Rahim, S. Ahmed, M.I. Malik, Calixarene coated gold nanoparticles as a novel therapeutic agent, Arab. J. Chem. 13 (2020) 3988–3996.
[4] W. Lee, D.G. Lee, A novel mechanism of fluconazole: fungicidal activity through dose-dependent apoptotic responses in *Candida albicans*, Microbiology 164 (2018) 194–204.
[5] W. Pasanphan, T. Rattanawongwiboon, S. Choofong, O. Guven, K.K. Katti, Irradiated chitosan nanoparticle as a water-based antioxidant and reducing agent for a green synthesis of gold nano platforms, Radiat. Phys. Chem. 106 (2015) 360–370.
[6] C. Qin, H. Li, X. Qi, L. Yi, J. Zhu, Y. Du, Water-solubility of chitosan and its antimicrobial activity, Carbohydr. Polym. 63 (2006) 367–374.
[7] W. Xu, Y. Xiao, P. Luo, L. Fan, Preparation and characterization of C-phycocyanin peptide grafted N-succinyl chitosan by enzyme method, Int. J. Biol. Macromol. 113 (2018) 841–848.
[8] Y. Kato, H. Onishi, Y. Machida, N-succinyl-chitosan as a drug carrier: water-insoluble and water-soluble conjugates, Biomaterials 25 (2004) 907–915.
[9] L.P. Sun, Y.M. Du, X.W. Shi, X. Chen, J.H. Yang, Y.M. Xu, A new approach tochemically modified carboxymethyl chitosan and study of itsmoisture-absorption and moisture-retention abilities, J. Appl. Polym. Sci. 102 (2006) 1303–1309.
[10] X. Niu, L. Zhu, L. Xi, L. Guo, H. Wang, An antimicrobial agent prepared by N-succinyl chitosan immobilized lysozyme and its application in strawberry preservation, Food Control 108 (2020), 106829, .
[11] A. Leiva, S. Bonardd, M. Pino, C. Saldías, G. Kortaberria, D. Radic, Improving the performance of chitosan in the synthesis and stabilization of gold nanoparticles, Eur. Polym. J. 68 (2015) 419–431.
[12] A.R. Futyra, M.K. Liskiewicz, V. Sebastian, S. Irusta, M. Arruebo, A. Kyzioł, G. Stochel, Development of noncytotoxic silver-chitosan nanocomposites for efficient control of biofilm forming microbes, RSC Adv. 7 (2017) 52398–52413.
[13] K. Aiedeh, M.O. Taha, Synthesis of chitosan succinate and chitosan phthalate and their evaluation as suggested matrices in orally administered, colon-specific drug delivery systems, Arch. Pharm. Pharm. Med. Chem. 332 (1999) 103–107.
[14] S. Bashir, Y.Y. Teo, S. Naeem, S. Ramesh, K. Ramesh, pH responsive N-succinyl chitosan/Poly(acrylamide-co-acrylic acid) hydrogels and *invitro* release of 5-fluorouracil, PLoS One 12 (2017) e0179250.
[15] F. Tang, L. Lv, F. Lu, B. Rong, Z. Li, B. Lu, K. Yu, J. Liu, F. Dai, D. Wu, G. Lan, Preparation and characterization of N-chitosan as a wound healing accelerator, Int. J. Biol. Macromol. 93 (2016) 1295–1303.
[16] P. Wayne, Reference Method for Broth Dilution Antifungal Susceptibility Testing of Yeasts, Approved Standard; CLSI Document M27-A2, 2002.
[17] R. Saravana Kumar, S.H.S. Dananjaya, M. De Zoysa, M. Yang, Enhanced antifungal activity of Ni-doped ZnO nanostructures under dark conditions, RSC Adv. 6 (2016) 108468–108476.
[18] S.H.S. Dananjaya, R.M.C. Udayangani, C. Oh, C. Nikapitiya, J. Lee, Mahanama De Zoysa, Green synthesis, physio-chemical characterization and anti-candidal function of a biocompatible chitosan gold nanocomposite as a promising antifungal therapeutic agent, RSC Adv. 7 (2017) 9182–9193.
[19] D.C.M. Kulatunga, S.H.S. Dananjaya, C. Nikapitiya, C.H. Kim, J. Lee, M. De Zoysa, Candida albicans infection model in Zebrafish (Danio rerio) for screening anticandidal drugs, Mycopathologia 184 (2019) 559–572.
[20] A.M. da Rocha, L.W. Kist, E.A. Almeida, D.G.H. Silva, C.D. Bonan, S. Altenhofen, C.G. Kaufmann Jr., M.R. Bogo, D.M. Barros, S. Oliveira, V. Geraldo, R.G. Lacerda, A.S. Ferlauto, L.O. Ladeira, J.M. Monserrat, Neurotoxicity in zebrafish exposed to carbon nanotubes: effects on neurotransmitters levels and antioxidant system, Comp. Biochem. Physiol. C Toxicol. Pharmacol. 218 (2019) 30–35.
[21] K.M. Aiedeh, H. Al Khatib, M.O. Taha, N. Al-Zoubi, Application of novel chitosan derivatives in dissolution enhancement of a poorly water soluble drug, Pharmazie 61 (2006) 306–311.
[22] L.O.A.N. Ramadhan, C.L. Radiman, V. Suendo, D. Wahyuningrum, S. Valiyaveettil, Synthesis and characterization of polyelectrolyte complex *N*-Succinylchitosan-chitosan for proton exchange membranes, Procedia Chem 4 (2012) 114–122.
[23] P. Mukhopadhyay, S. Maity, S. Mandal, A.S. Chakraborti, A.K. Prajapati, P.P. Kundu, Preparation, characterization and in vivo evaluation of pH sensitive, safe quercetin-succinylated chitosan-alginate core-shell-corona nanoparticle for diabetes treatment, Carbohydr. Polym. 182 (2018) 42–51.
[24] Y. Monsalve, L. Sierra, B.L. Lopez, Preparation and characterization of succinyl- chitosan nanoparticles for drug delivery, Macromol. Symp. 354 (2015) 91–98.
[25] J.Q. Zhou, J.W. Wang, Immobilization of alliinase with a water soluble-insoluble reversible *N*-succinyl-chitosan for allicin production, Enzym. Microb. Technol. 45 (2009) 299–304.
[26] D.S. Salem, M.A. Sliem, M.E. Sesy, S.A. Shouman, Y. Badr, Improved chemo-photothermal therapy of hepatocellular carcinoma using chitosan-coated gold nanoparticles, J. Photochem. Photobiol. B 182 (2018) 92–99.
[27] S.R. Bhattarai, R. Bahadur, S. Aryal, N. Bhattarai, S.Y. Kim, H.K. Yi, P.H. Hwang, H.Y. Kim, Hydrophobically modified chitosan/gold nanoparticles for DNA delivery, J. Nanopart. Res. 10 (2008) 151–162.
[28] I.A. Wani, T. Ahmad, Size and shape dependant antifungal activity of gold nanoparticles: a case study of Candida, Colloids Surf. B: Biointerfaces 101 (2013) 162–170.
[29] C. Yan, D. Chen, J. Gu, J. Qin, Nanoparticles of 5-fluorouracil (5-FU) loaded N-succinyl-chitosan (Suc-Chi) for cancer chemotherapy: preparation, characterization - in-vitro drug release and anti-tumour activity, J. Pharm. Pharmacol. 58 (2006) 1177–1181.
[30] W. Namangkalakul, S. Benjavongkulchai, T. Pochana, A. Promchai, W. Satitviboo, S. Howattanapanich, R. Phuprasong, N. Ungvijanpunya, D. Supakanjanakanti, T. Chaitrakoonthong, S. Muangsawat, P. Thanyasrisung, Oranart Matangkasombut, Activity of chitosan antifungal denture adhesive against common Candida species and Candida albicans adherence on denture base acrylic resin, J. Prosthet. Dent. 123 (2020) 181.e1–181.e7.
[31] H. Rahimi, S. Roudbarmohammadi, H. Delavari, M. Roudbary, Antifungal effects of indolicidin-conjugated gold nanoparticles against fluconazole-resistant strains of Candida albicans isolated from patients with burn infection, Int. J. Nanomedicine 14 (2019) 5323–5338.
[32] M. Seong, D.G. Lee, Reactive oxygen species-independent apoptotic pathway by gold nanoparticles in Candida albicans, Microbiol. Res. 207 (2018) 33–40.
[33] L.C. Crowley, A.P. Scott, B.J. Marfell, J.A. Boughaba, G. Chojnowski, N.J. Waterhouse, Measuring cell death by propidium iodide uptake and flow cytometry, Cold Spring Harb Protoc 1 (7) (2016)https://doi.org/10.1101/pdb.prot087163.
[34] C. Chellamuthu, R. Balakrishnan, P. Patel, R. Shanmuganathan, A. Pugazhendhi, K. Ponnuchamy, Gold nanoparticles using red seaweed *Gracilaria verrucosa*: green synthesis, characterization and biocompatibility studies, Process Biochem. 80 (2019) 58–63.
[35] G.R. Tortella, O. Rubilar, N. Duran, M.C. Diez, M. Martínez, J. Parada, A.B. Seabra, Silver nanoparticles: toxicity in model organisms as an overview of its hazard for human health and the environment, J. Hazard. Mater. 390 (2020), 121974, .
[36] C.C. Chao, P.C. Hsu, C.F. Jen, I.H. Chen, C.H. Wang, H.C. Chan, P.W. Tsai, K.C. Tung, C.H. Wang, C.Y. Lan, Y.J. Chuang, Zebrafish as a model host for Candida albicans infection, Infect. Immun. 78 (2010) 2512–2521.
[37] F.C. Odds, Candida and candidosis: a review and bibliography, J. Basic Microbiol. 30 (1988) 382–383.
[38] Dananjaya S.H.S, Thu Thao N.T., Wijerathna H.M.S.M., Jisoo Lee., Edussuriy M., Dongrack Choi., Saravana Kumar R.,, In vitro and in vivo anticandidal efficacy of green synthesized gold nanoparticles using *Spirulina maxima* polysaccharide, Process Biochem. 92 (2020) 138–148, https://doi.org/10.1016/j.procbio.2020.03.003 38.